Degeneracy between Interacting Dark Energy and Primordial Non-Gaussianity

Mahmoud Hashim

Centre for Theoretical Physics

The British University in Egypt

The BRITISH UNIVERSITY IN EGYPT
CENTRE FOR THEORETICAL PHYSICS

Workshop on Astro-particles and Gravity, Cairo U., 20-22 Sept, 2022

Centre for Theoretical Physics . . . The British University in Egypt

Structure Formation

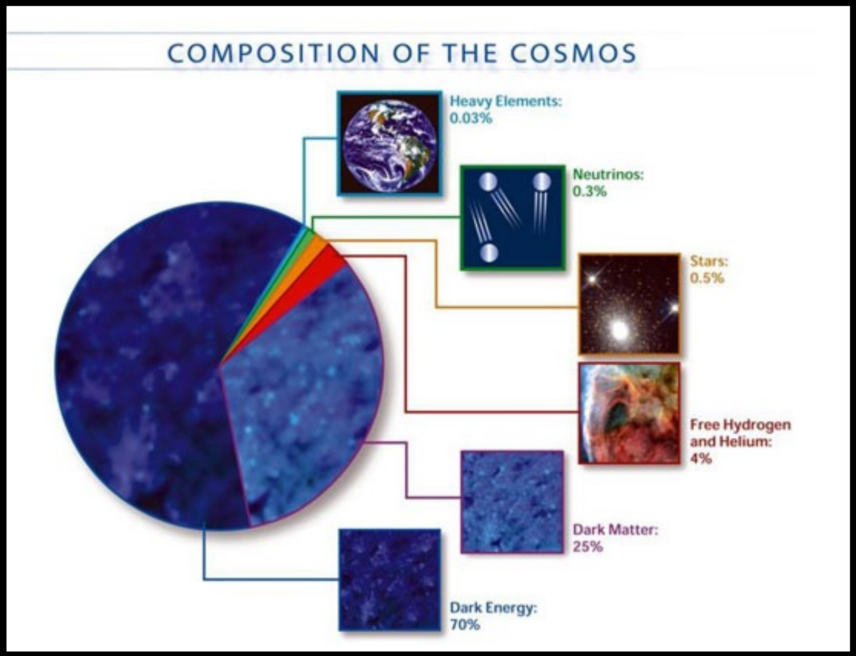

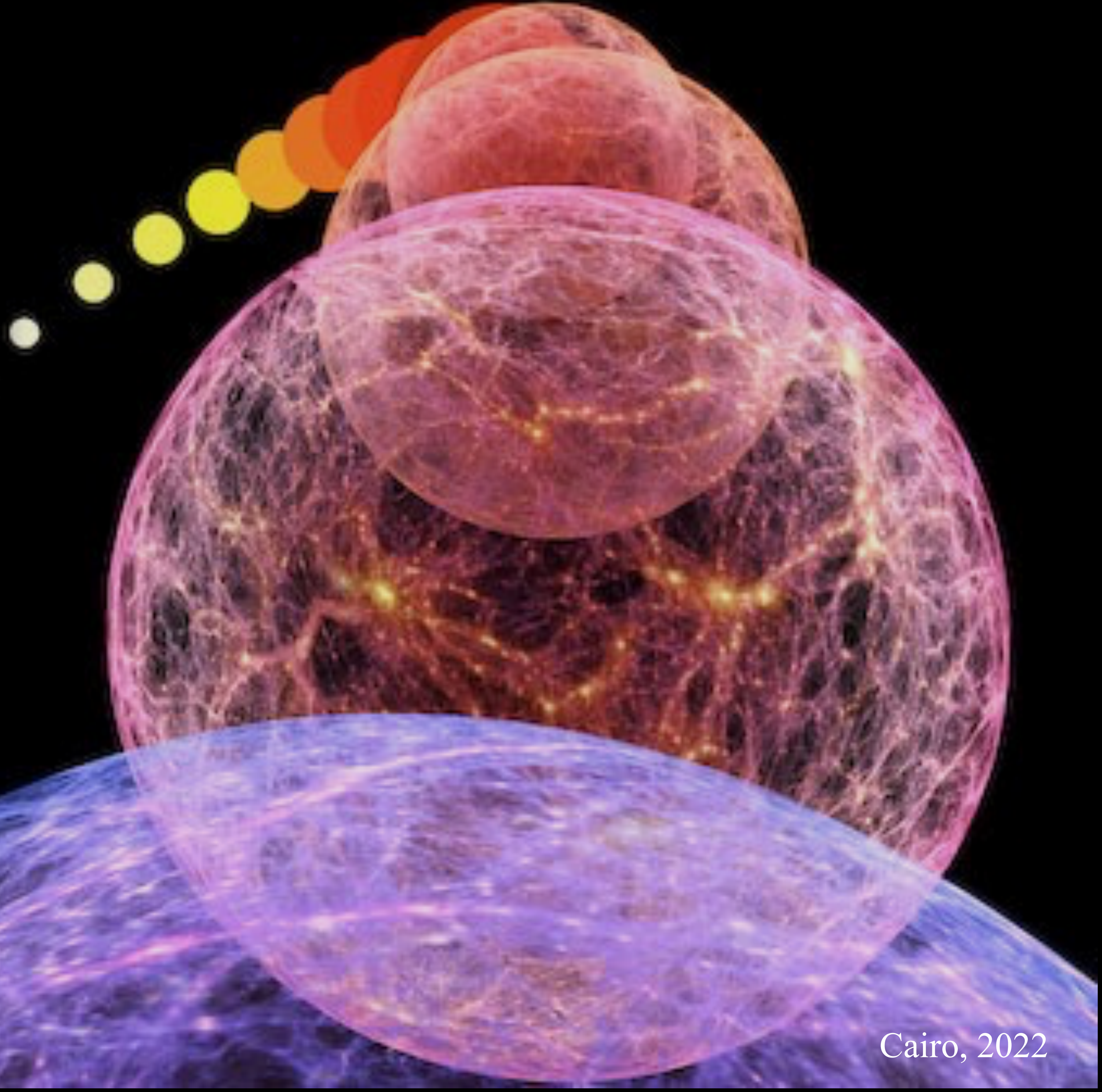

Cairo, 2022

primordial non-Gaussianity

(Inflation)

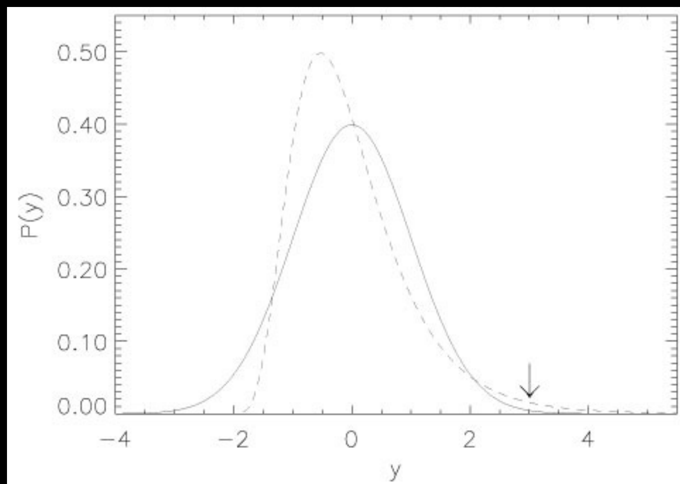

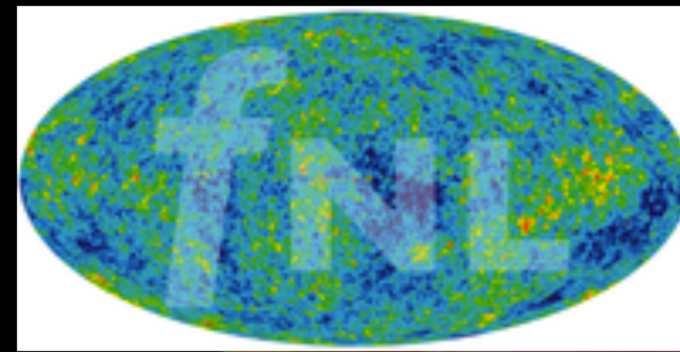

Dark Sector

(Dark Matter & Dark Energy)

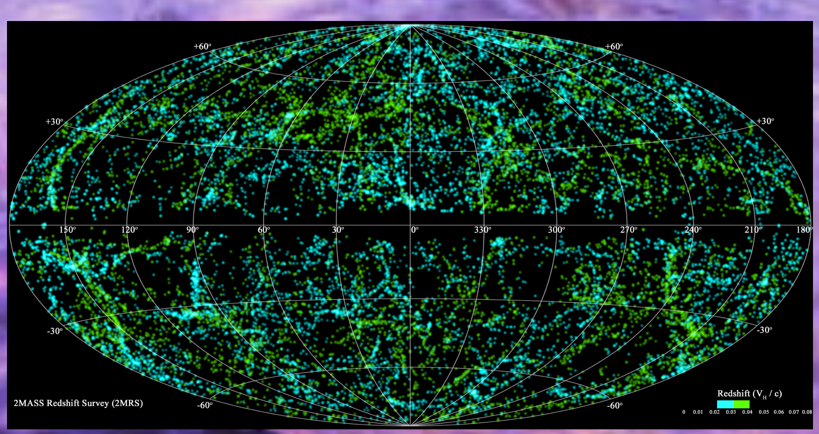

Cairo, 2022

Interacting Dark Energy

Interaction between Dark Energy and Dark Matter is a theoretical possibility that may help to solve the coincidence problem.

Dark energy and dark matter interact via energy-momentum exchange.

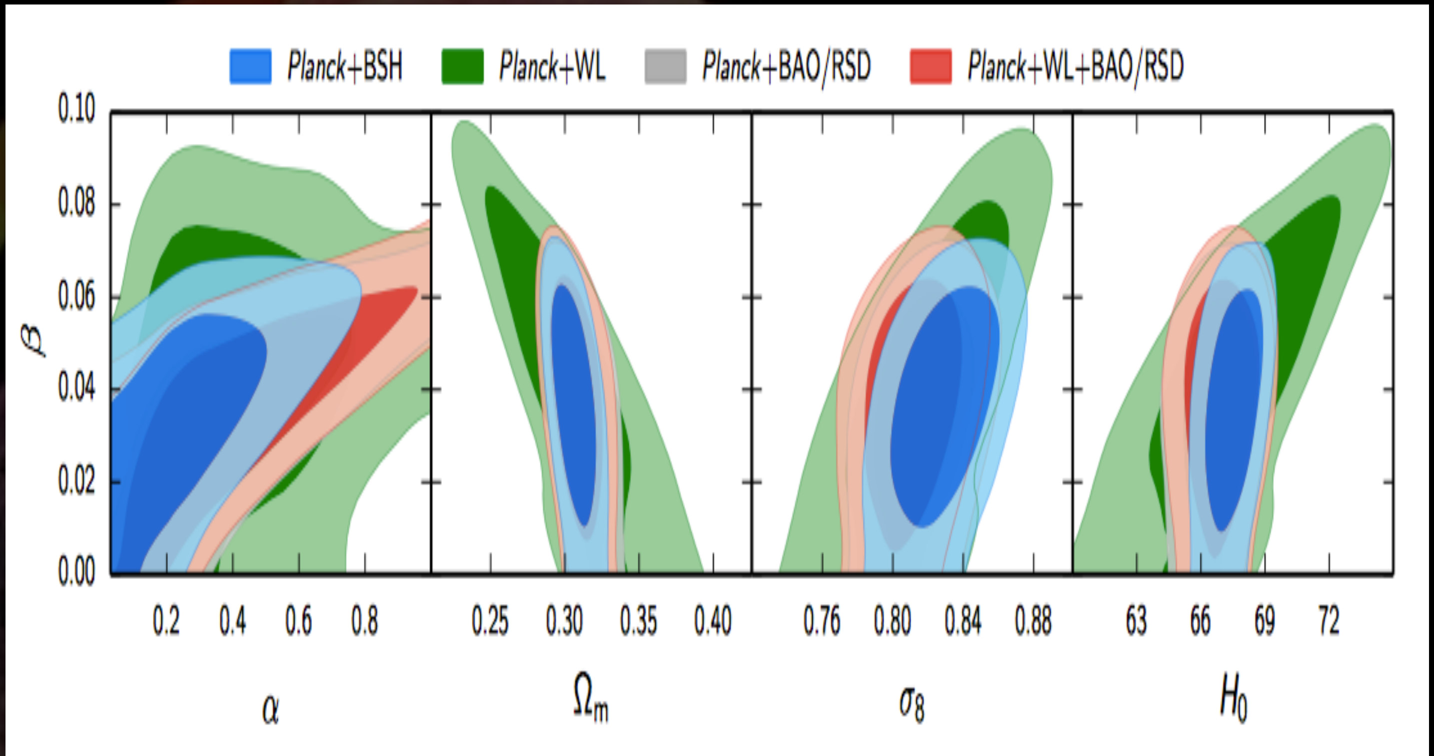

Planck Collaboration 2015 (arXiv:1502.01590)

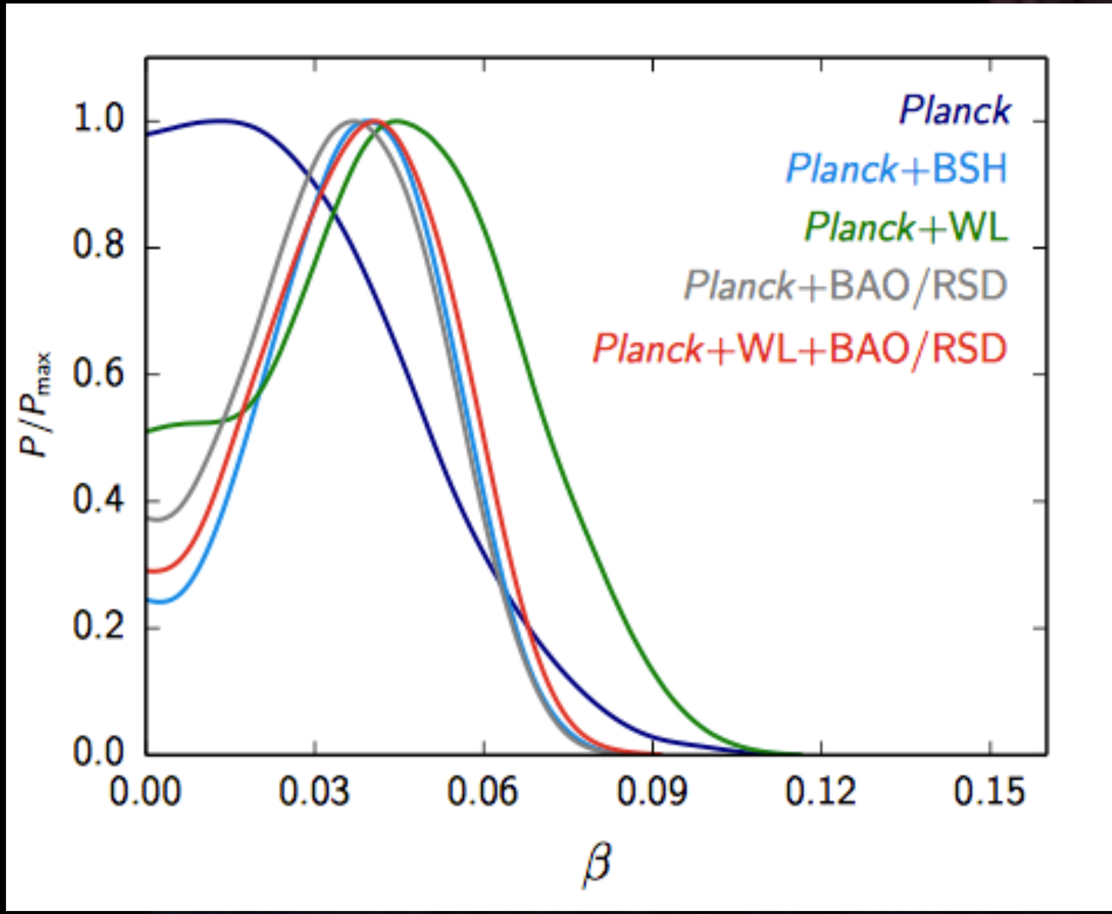

The transfer of energy-momentum between dark matter and dark energy is not ruled out by current observations.

Cairo, 2022

Primordial Non-Gaussianity

- Primordial Non-Gaussianity(PNG) is used to discriminate between different inflation models.
- Planck has shown that PNG is not large.
- In order to further and detect small PNG, we need larger galaxy surveys.

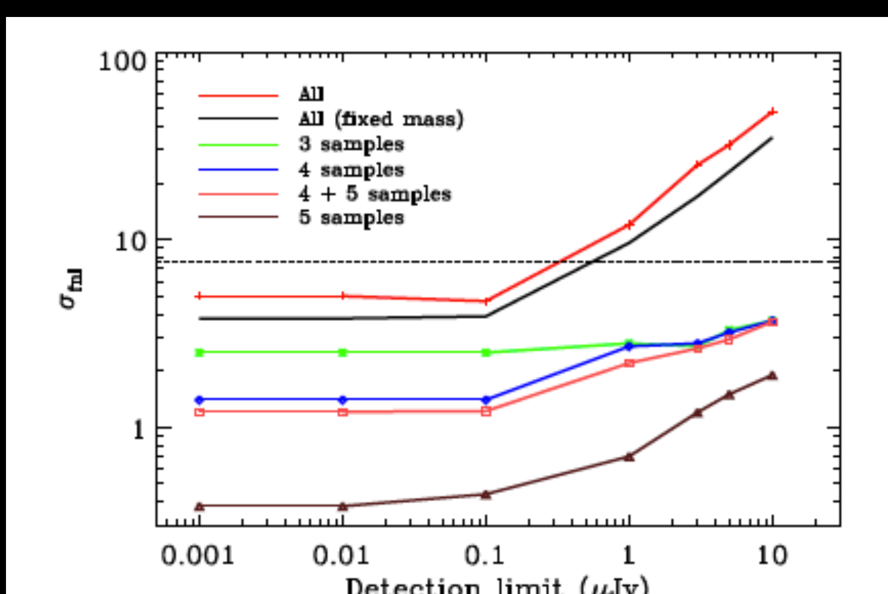

Forecast for SKA continuum surveys, Ferramacho et al. 2014

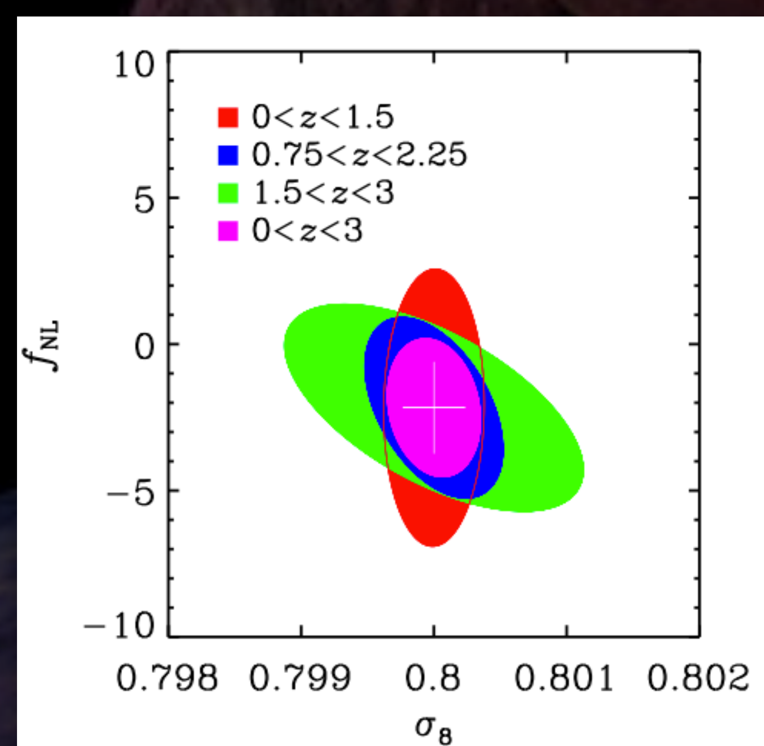

Forecast for SKA HI galaxy redshift surveys, Camera et al. 2014

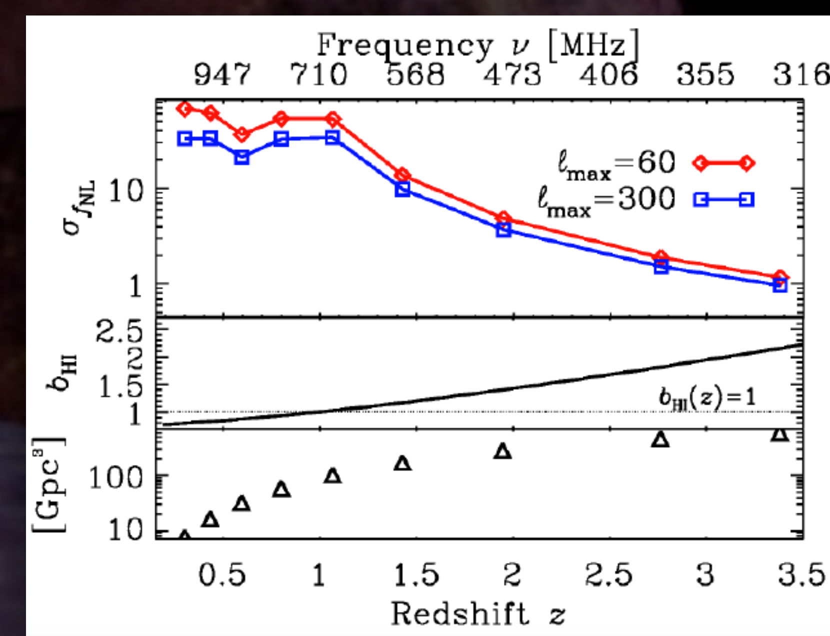

Forecast for SKA HI intensity mapping surveys, Camera et al. 2013

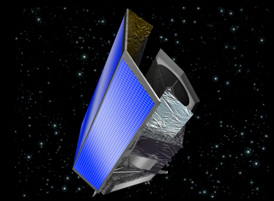

Cosmic/Parameter Degeneracy

LSS$_{(\text{EUCLID, SKA, ..})}$ Λ + CDM vs $\beta(\phi$ + CDM) + fNL

$$f_{obs} \xrightarrow{\text{likelihood analysis}} f_{thr}(p_i=\{H_0,\Omega_{m,\Lambda,..},n_s, A_s,\dots\}) \simeq f'_{thr}(p_i=\{H_0,\Omega_{m,\phi,..},w_\phi, \beta, n_s, A_s, fNL,\dots\})$$

Observational Probes

Background

Angular diameter distance; BAO
Distance Modulus; SNIa, …

Perturbed

linear(LPT)

Linear Power Spectrum Bispectrum?

nonlinear(N-Body)

Halo Statistics Nonlinear Power Spectrum
Halo Structural Properties Halo Bias

Cairo, 2022

$$\rho'_A + 3(1+w_A)\rho_A = \frac{aQ_A}{\mathcal{H}} \qquad Q_x = -Q_m.$$

$$Q_x = \Gamma\rho_x = -Q_m$$

Interaction term

Continuity Equation

Energy Transfer

$$\nabla^2\Phi = \frac{3}{2}\mathcal{H}\sum_A \Omega_A[\delta_A - 3\mathcal{H}(1+w_A)v_A],$$

$$\Delta_A = \delta_A + \frac{\rho'_A}{\rho_A}v_A.$$

Poisson Equation

Interaction perturbation source term

$$\nabla^2\Phi = \frac{3}{2}\mathcal{H}^2\left(\sum_A \Omega_A\Delta_A - Q^\Phi\right),$$

$$Q^\Phi = \frac{a}{\rho_t}\sum_A Q_A v_A = \frac{a}{\rho_t}Q_x(v_x - v_m).$$

Cairo, 2022

$$D_m(k,a) = \frac{\Delta_m(k,a)}{\Delta_{md}(k)} a_d,$$

Matter Growth factor

$$D_m = \frac{\Omega_{md}}{\Omega_m(1+\mu)} \left[\frac{a_d \mathcal{H}_d^2}{a\mathcal{H}^2} D_\Phi - \mu \frac{\Omega_x}{\Omega_{xd}} D_x - B \frac{a_d \mathcal{H}_d^2}{T(k) k^{n_s/2}} Q^\Phi \right],$$

$$Q^\Phi = a\Gamma\Omega_x(v_x - v_m).$$

Dark Energy source term

Scale-dependent interaction source term

Cairo, 2022

Linear Perturbation Theory

Λ + CDM vs β(ϕ + CDM) + fNL

$$b(k, z) = b_g(z) + \Delta b(k, z),$$

$$\Delta b = 3 f_{\rm NL} (b - 1) \frac{\delta_c H_0^2 \Omega_{m0}}{k^2 T D_m},$$

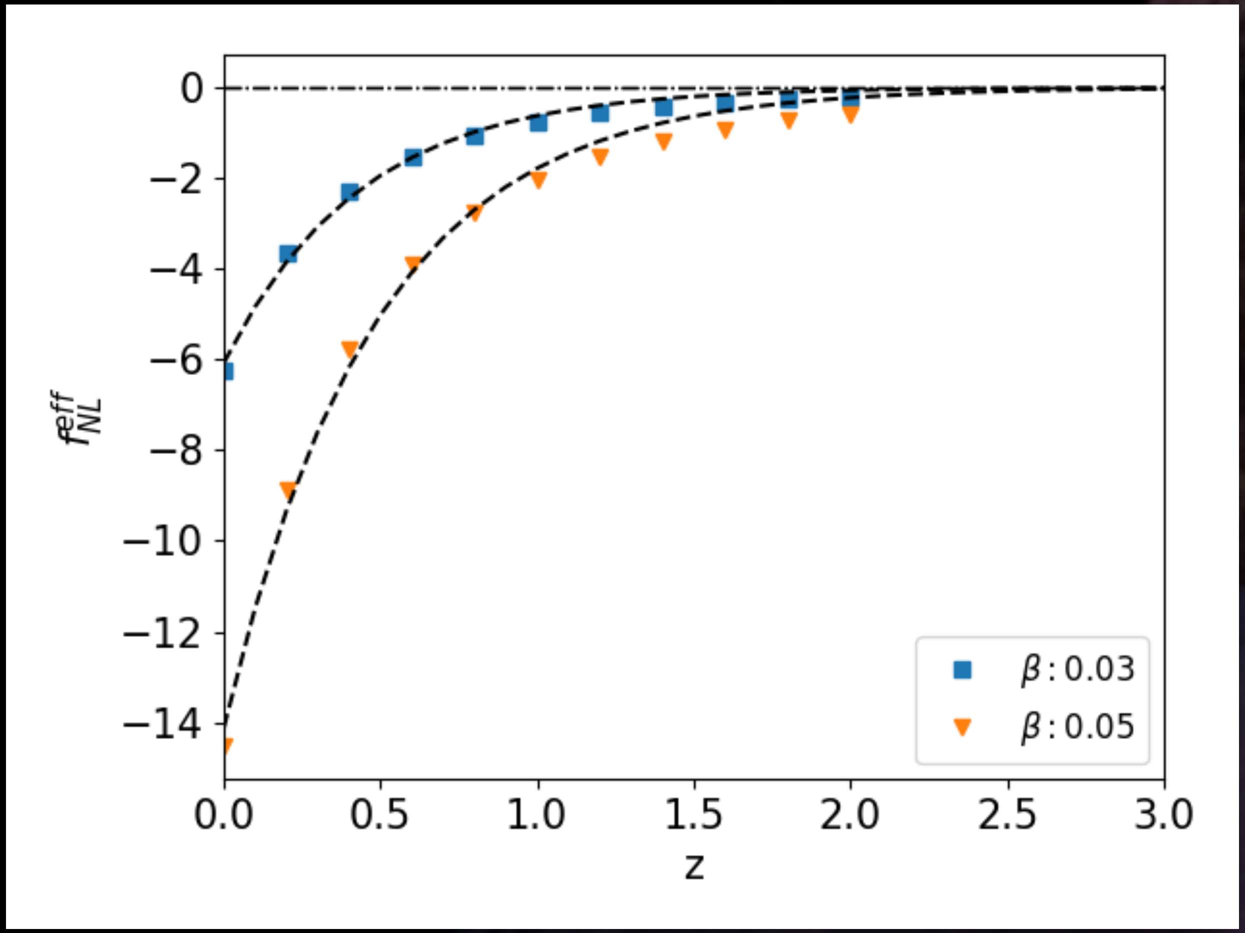

$$f_{\rm NL}^{\rm eff} = a e^{-bz} \beta,$$

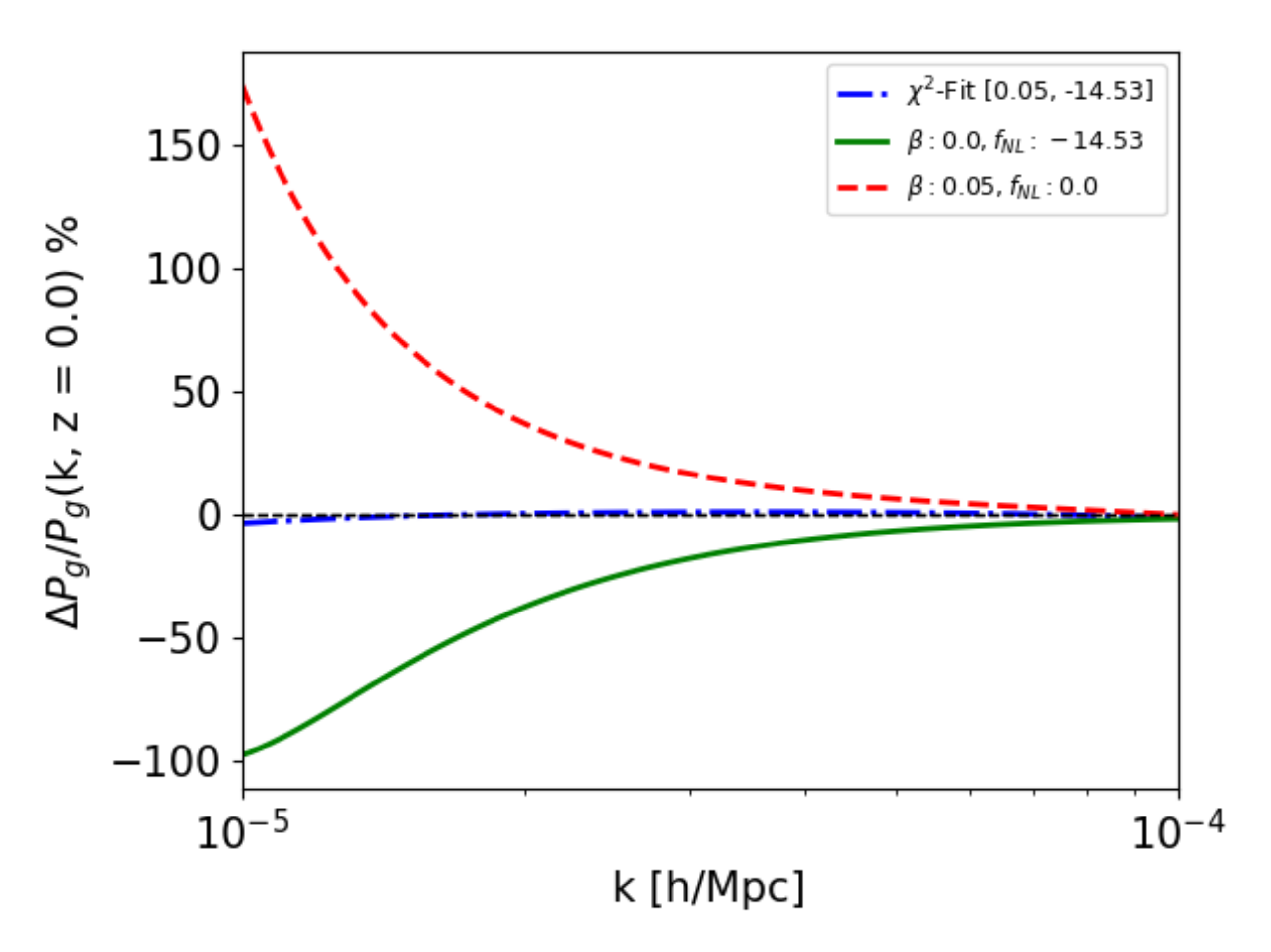

$$P_g(k, a) = b^2 P_m(k, a),$$

$$P_m(k, a) = \frac{9A^2}{50\pi^3 H_0^n} k^n T(k)^2 \left[\frac{D_m(k, a)}{D_{\Phi 0}(k)}\right]^2.$$

arXiv:1409.4933

Cairo, 2022

N-Body Simulation

Λ + CDM vs β(ϕ + CDM) + fNL

Initial Conditions

Gaussian particle distribution.

Add non-Gaussianity

$$\Phi = \phi + f_{\rm NL}(\phi^2 - \langle \phi^2 \rangle),$$

Initial power spectrum.

Modified amplitude but same shape.

Structure Formation

- Modified expansion rate.
- Mass variation.
- Extra velocity-dependent acceleration.
- Fifth force.

$$\tilde{H} \equiv H\left(1 - \frac{\beta(\phi)}{M}\frac{\dot{\phi}}{H}\right) \qquad f(a) \sim \Omega_M^{\gamma}\left(1 + \gamma\frac{\Omega_{\rm CDM}}{\Omega_M}\epsilon_c\beta_c^2\right)$$

$$\tilde{G}_c = G_N[1 + 2\beta^2(\phi)], \quad \tilde{M}_c \equiv M_c e^{-\int \beta(\phi)\frac{\mathrm{d}\phi}{\mathrm{d}a}\mathrm{d}a} \quad .$$

N-Body Simulation

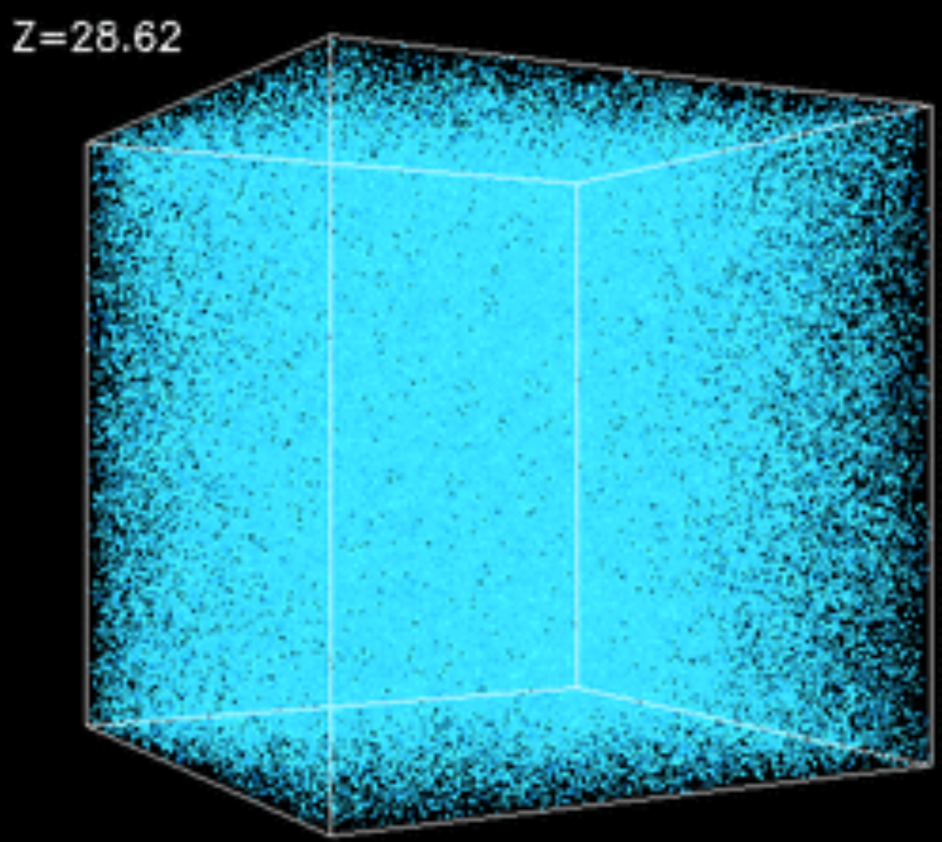

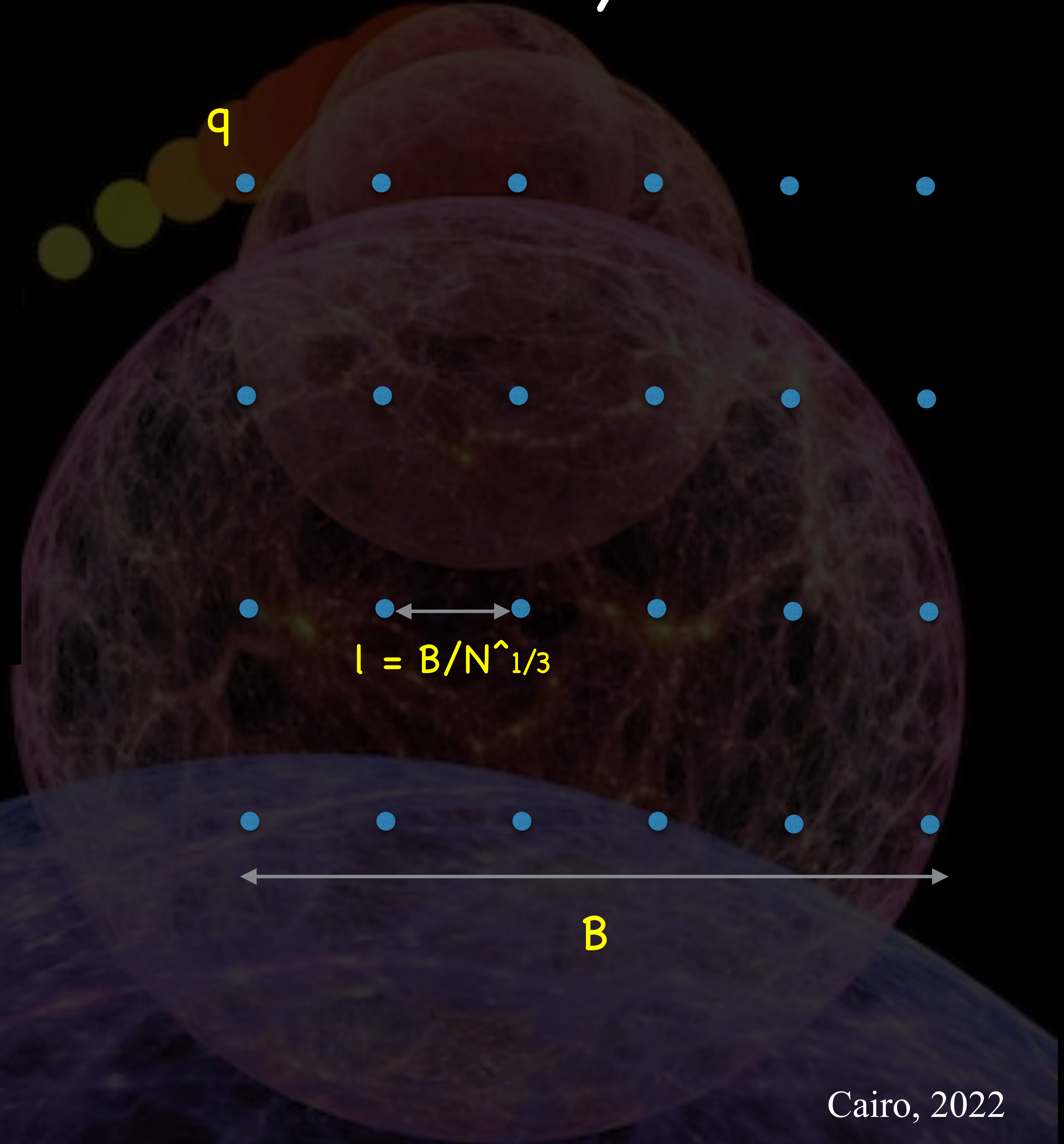

N-Body Simulation

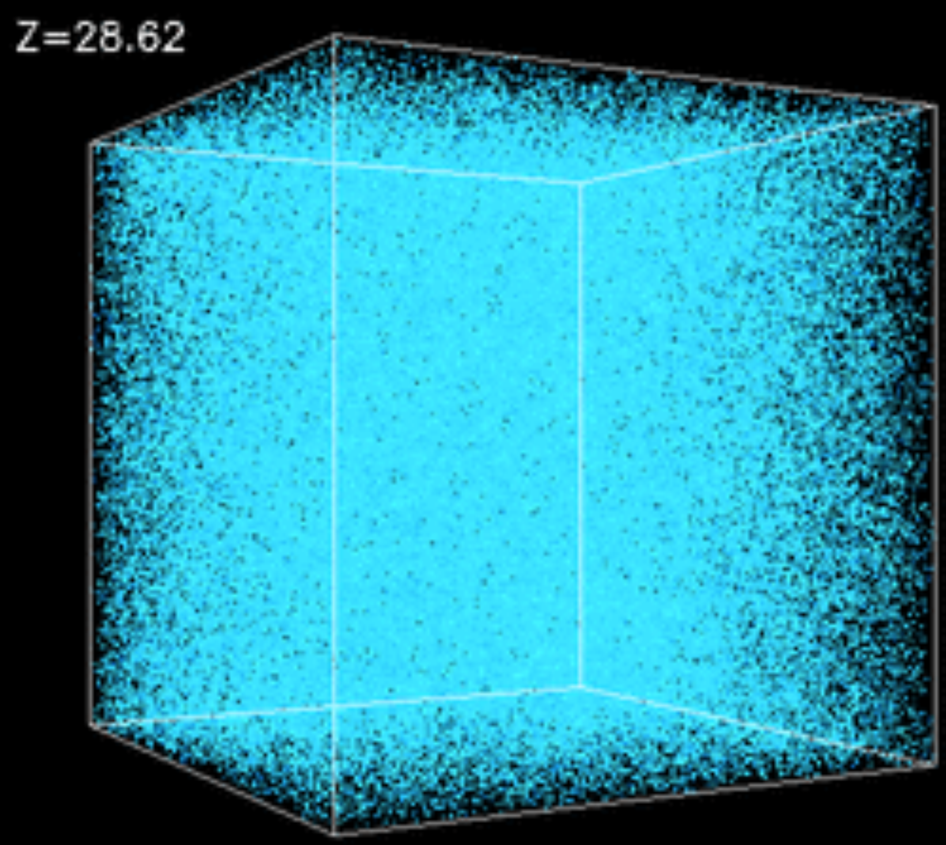

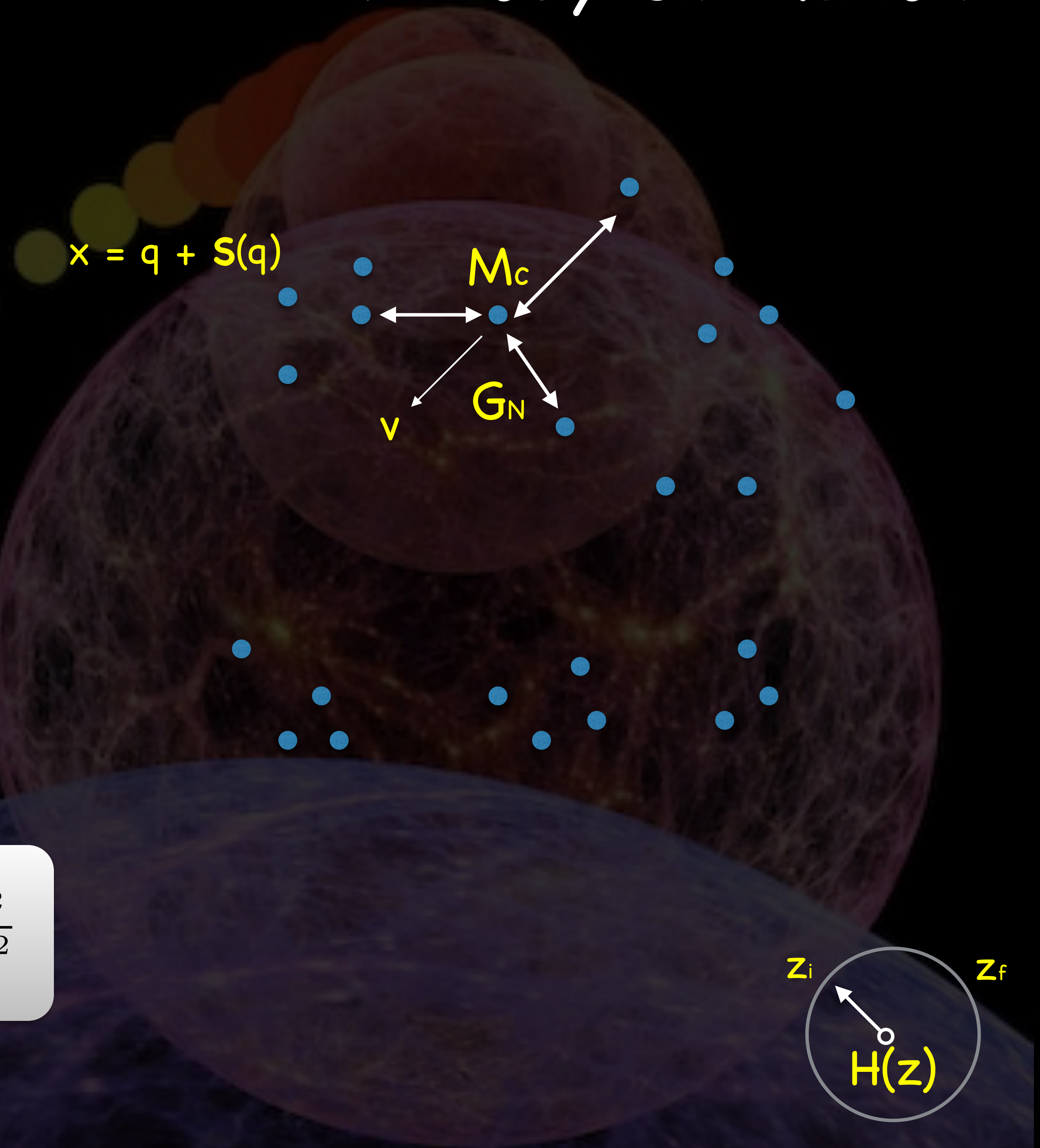

+ ICs (ZA, 2LPT)

$$\boldsymbol{v}(\boldsymbol{k},a) = i f(a) a H \delta(\boldsymbol{k},a) \frac{\boldsymbol{k}}{k^2}$$

N-Body Simulation

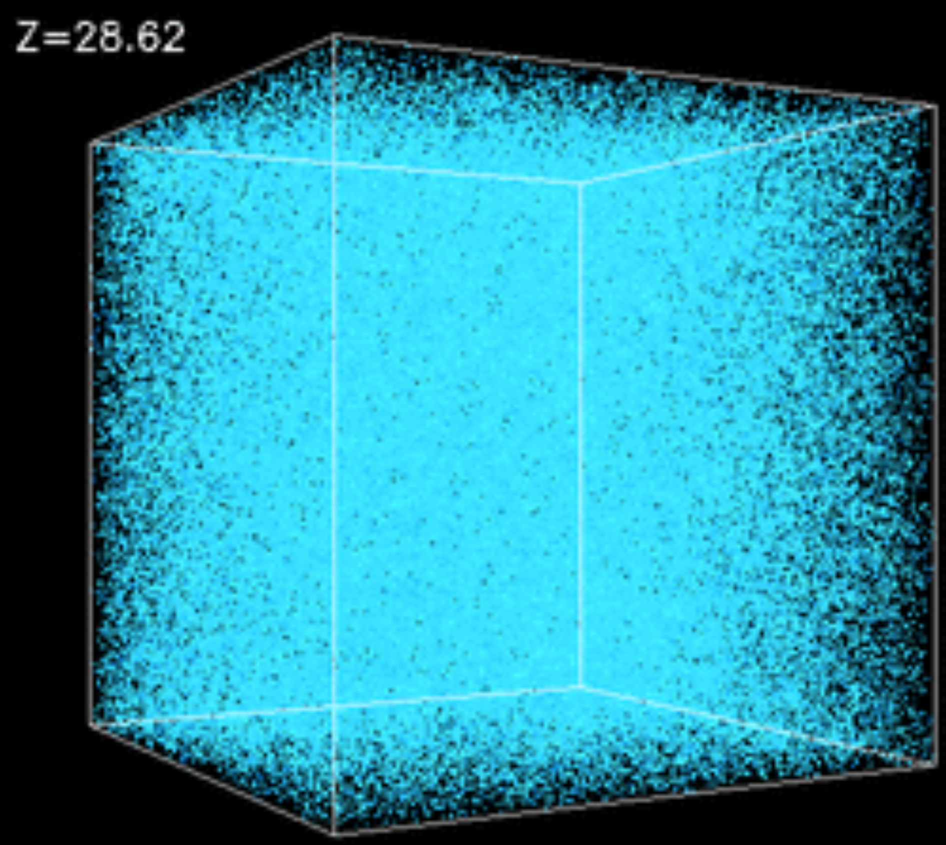

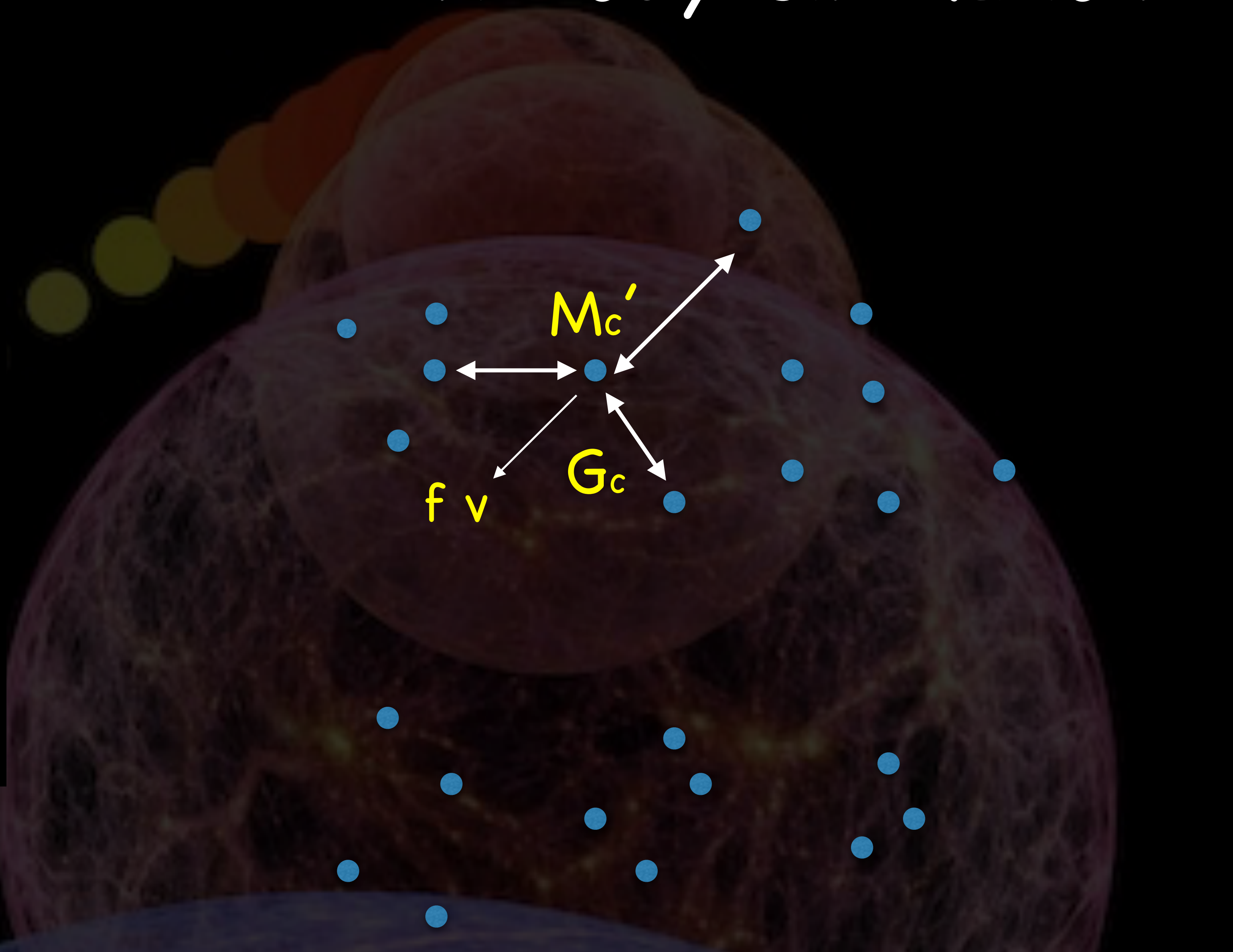

+ ICs (ZA, 2LPT)

+ Interaction

$$\tilde{H} \equiv H\left(1 - \frac{\beta(\phi)}{M}\frac{\dot{\phi}}{H}\right) \qquad f(a) \sim \Omega_M^{\gamma}\left(1 + \gamma\frac{\Omega_{\rm CDM}}{\Omega_M}\epsilon_c\beta_c^2\right)$$

$$\tilde{G}_c = G_N[1 + 2\beta^2(\phi)], \quad \tilde{M}_c \equiv M_c e^{-\int \beta(\phi)\frac{{\rm d}\phi}{{\rm d}a}{\rm d}a} \quad .$$

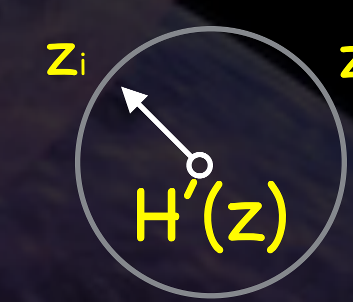

N-Body Simulation

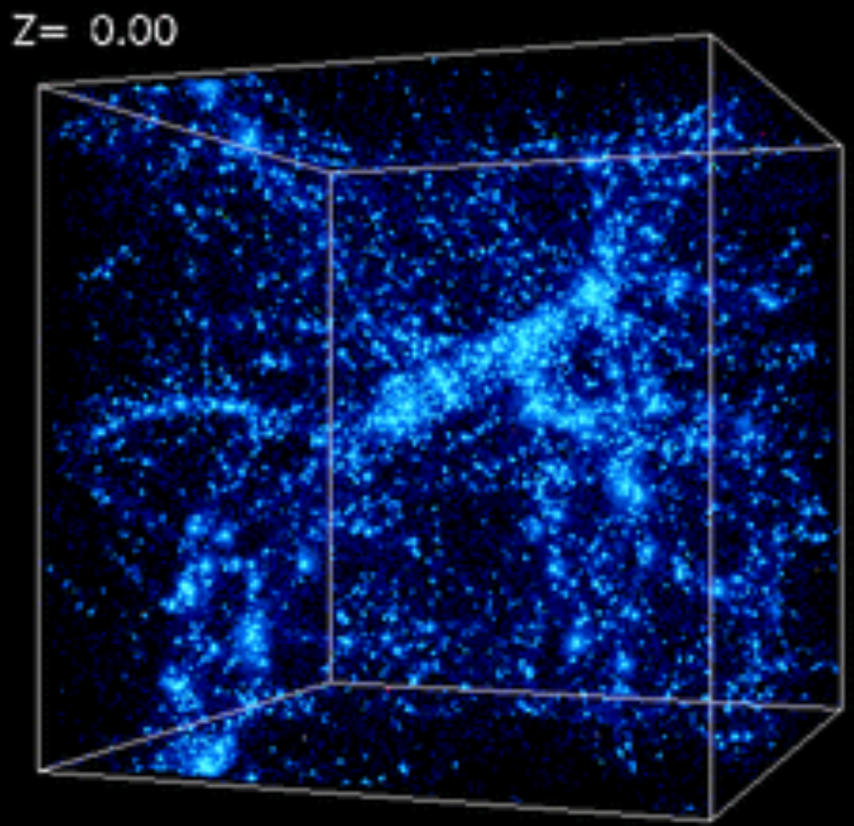

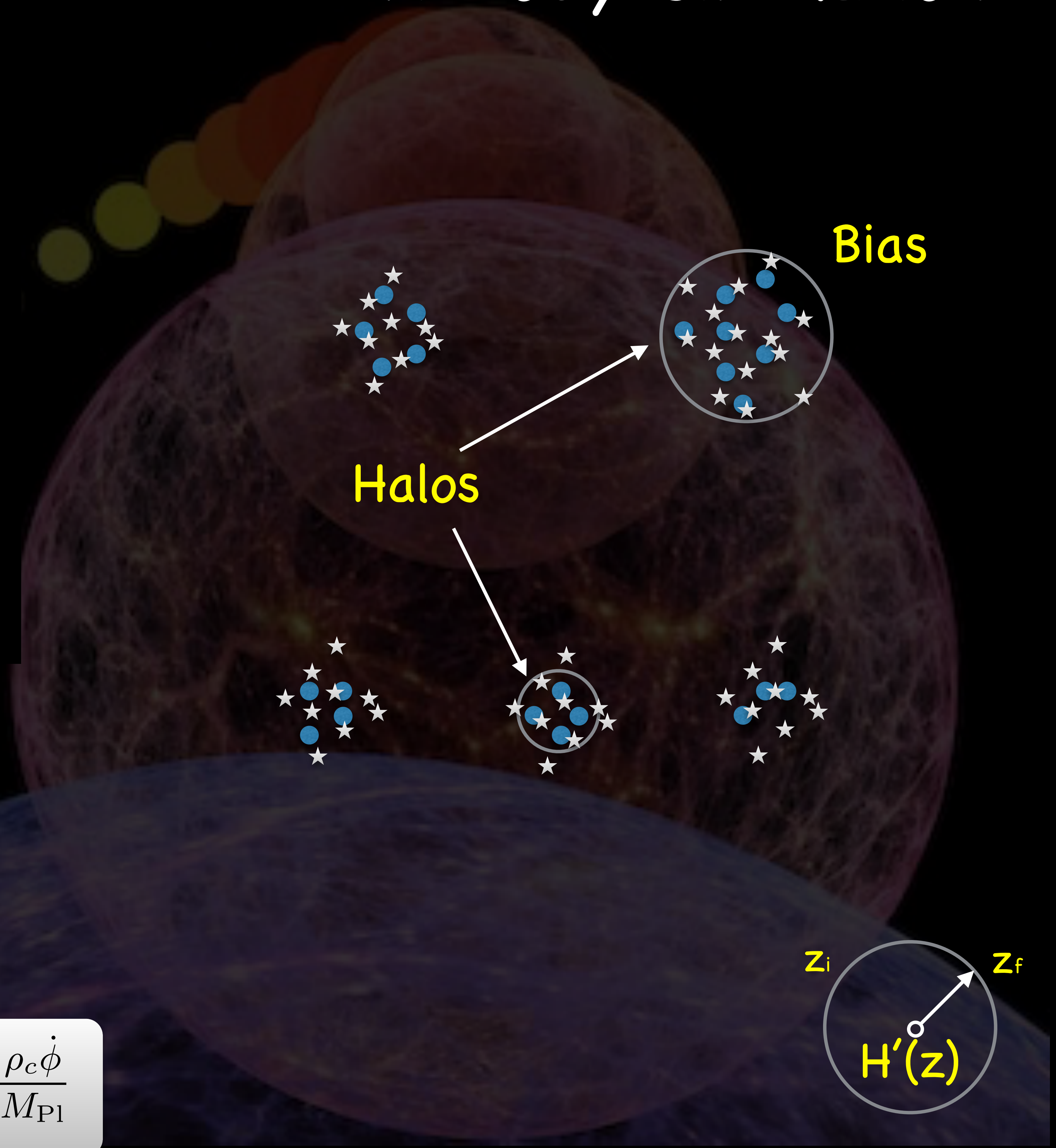

+ ICs (ZA, 2LPT)

+ Interaction

+ Evolution

$$\dot{\rho}_c + 3H\rho_c = -\sqrt{\frac{2}{3}}\beta_c(\phi)\frac{\rho_c\dot{\phi}}{M_{\rm Pl}}$$

N-Body Simulation

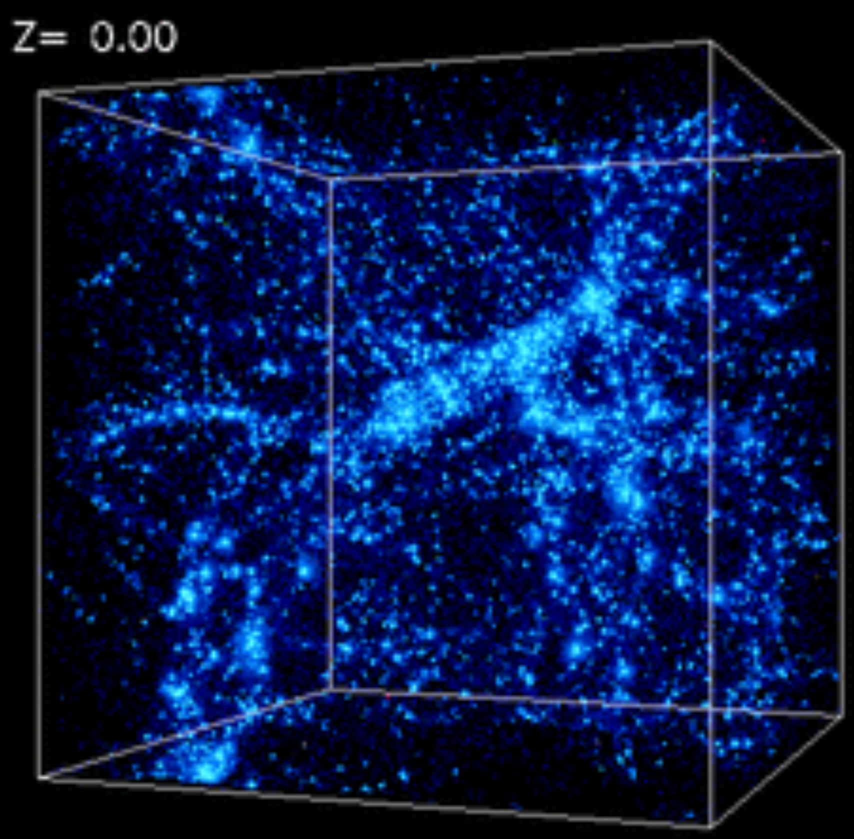

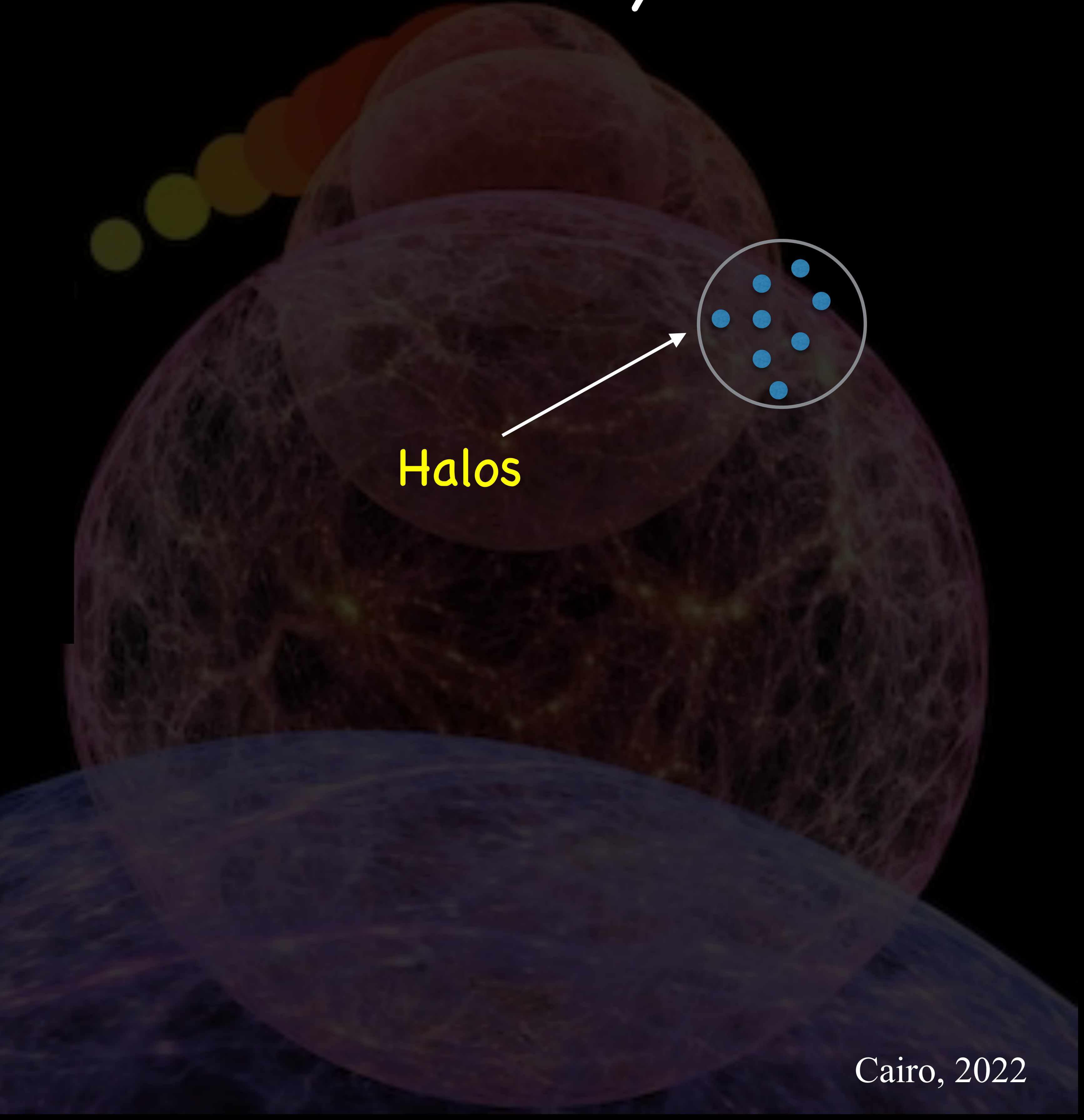

Cairo, 2022

N-Body Simulation

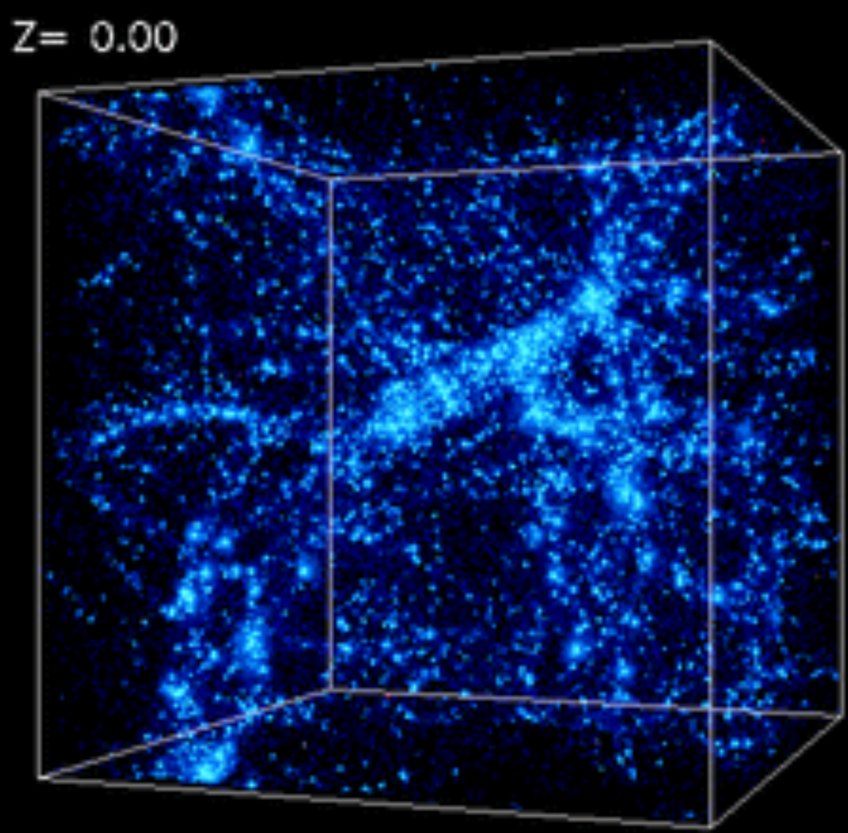

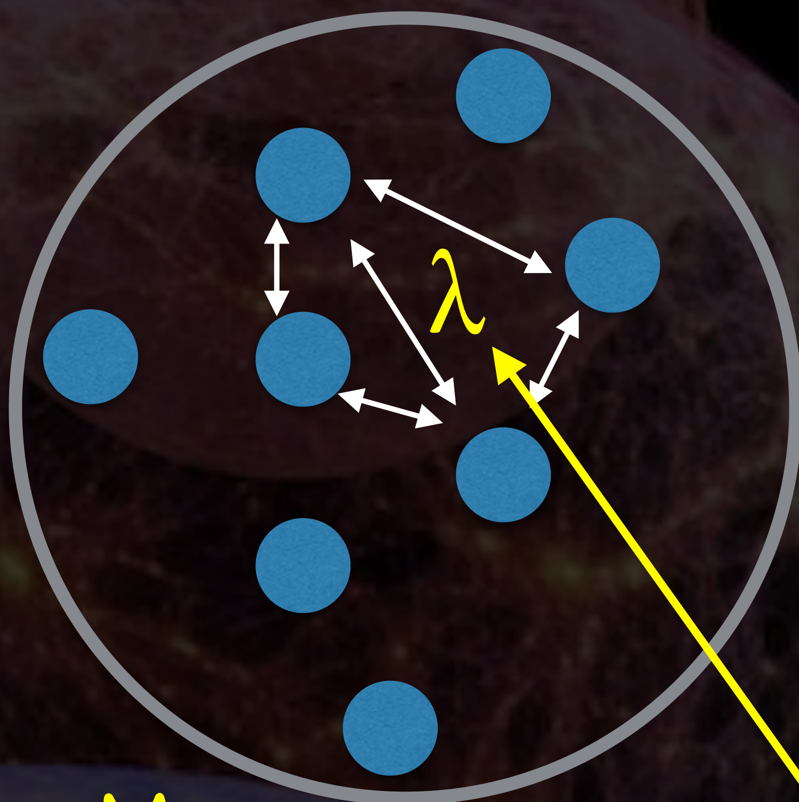

$\lambda \equiv b \cdot l$

Halos (HMf)

$$\frac{dn}{d\log M} = \frac{M}{L^3}\frac{\Delta N}{\Delta \log M}$$

Cairo, 2022

N-Body Simulation

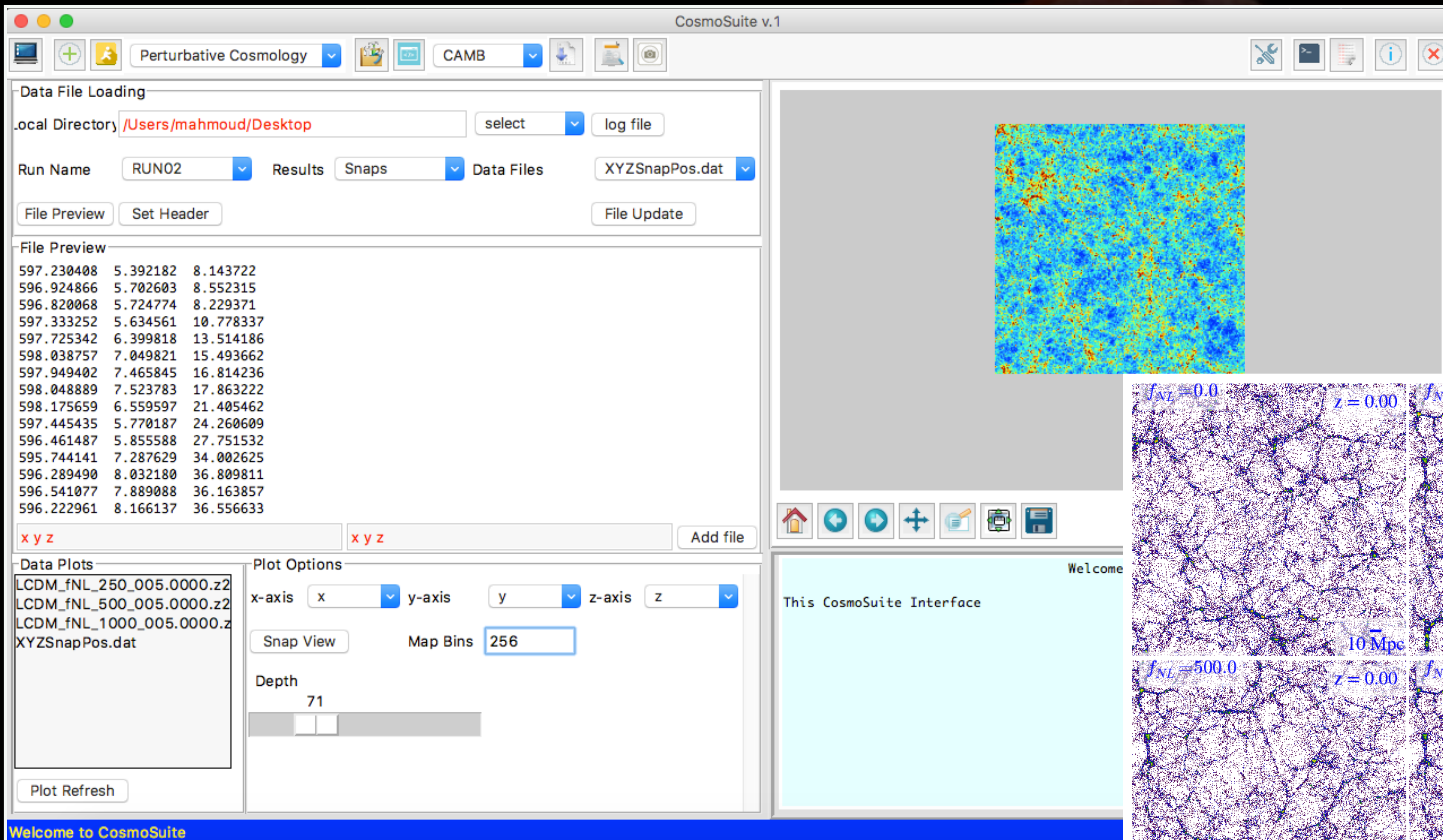

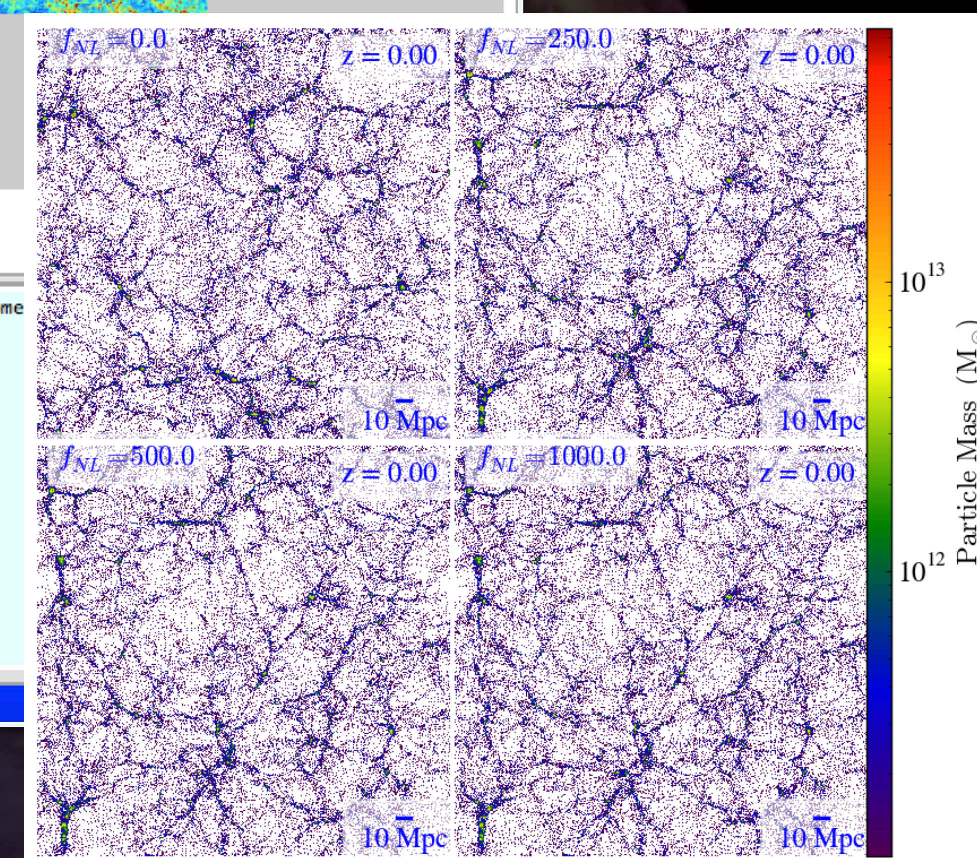

CosmoSuite

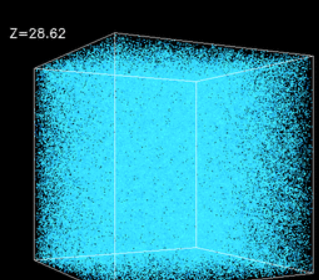

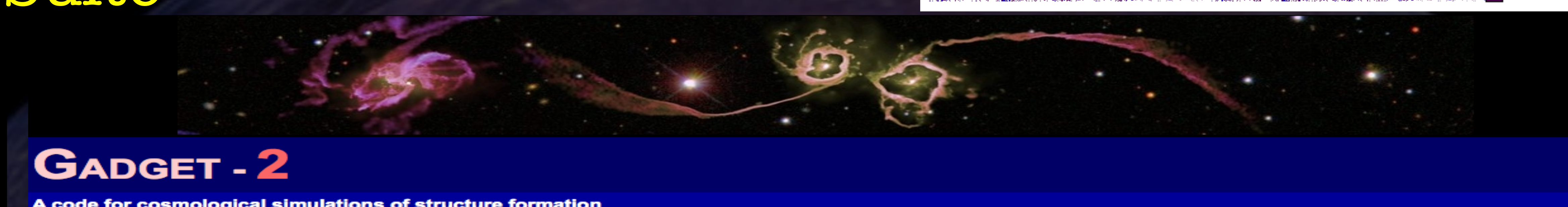

Nonlinear power spectrum

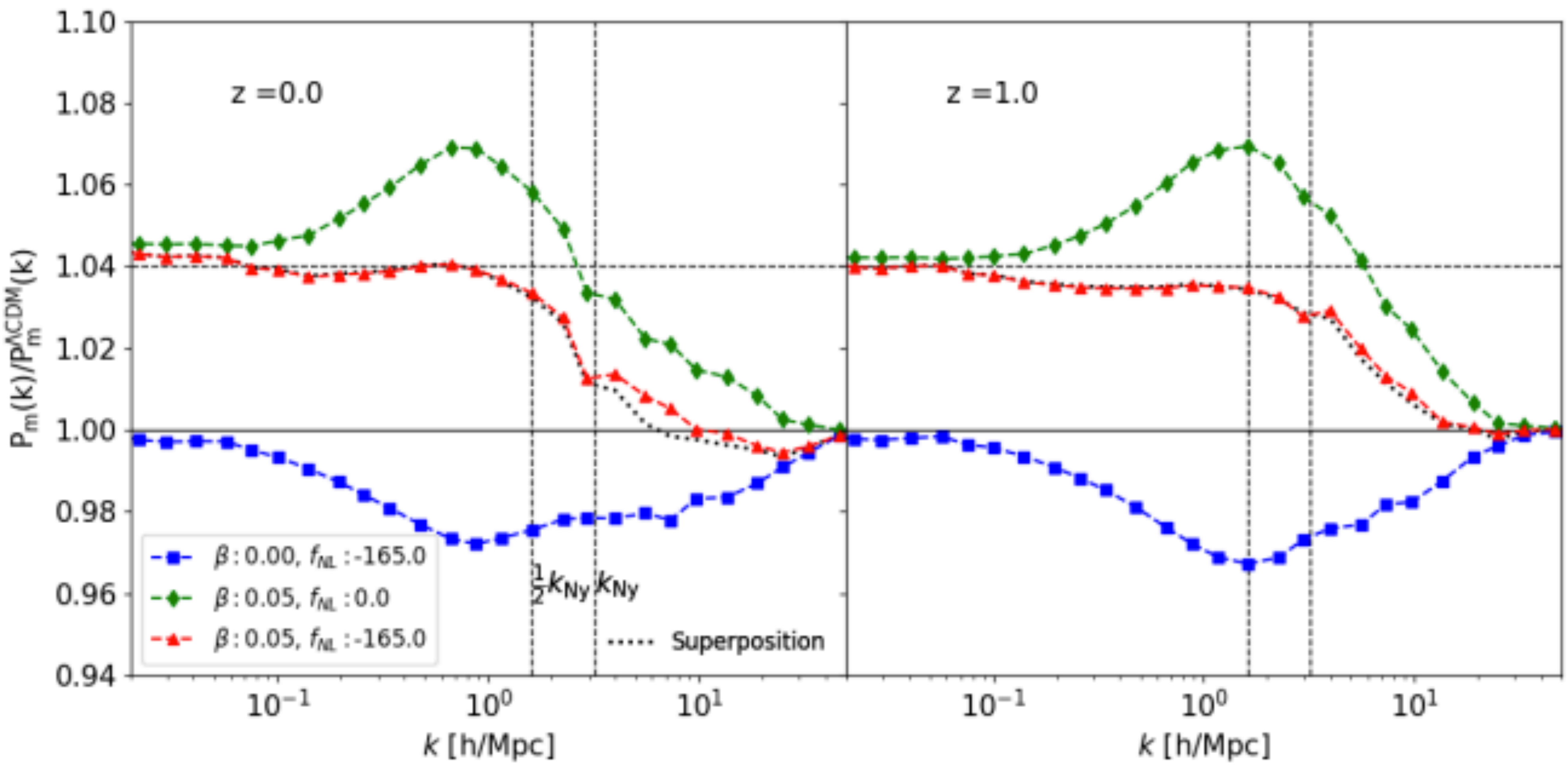

Figure 3. The non-linear matter power spectrum with IDE, PNG and their combination, relative to the reference ΛCDM spectrum, at $z = 0$ (left panel) and $z = 1$ (right panel). The dotted black curve shows the superposition spectra (IDE-only + PNG-only). The black dashed vertical lines show the Nyqvist frequency and half of it.

arXiv:1806.02356

Cairo, 2022

Halo Bias

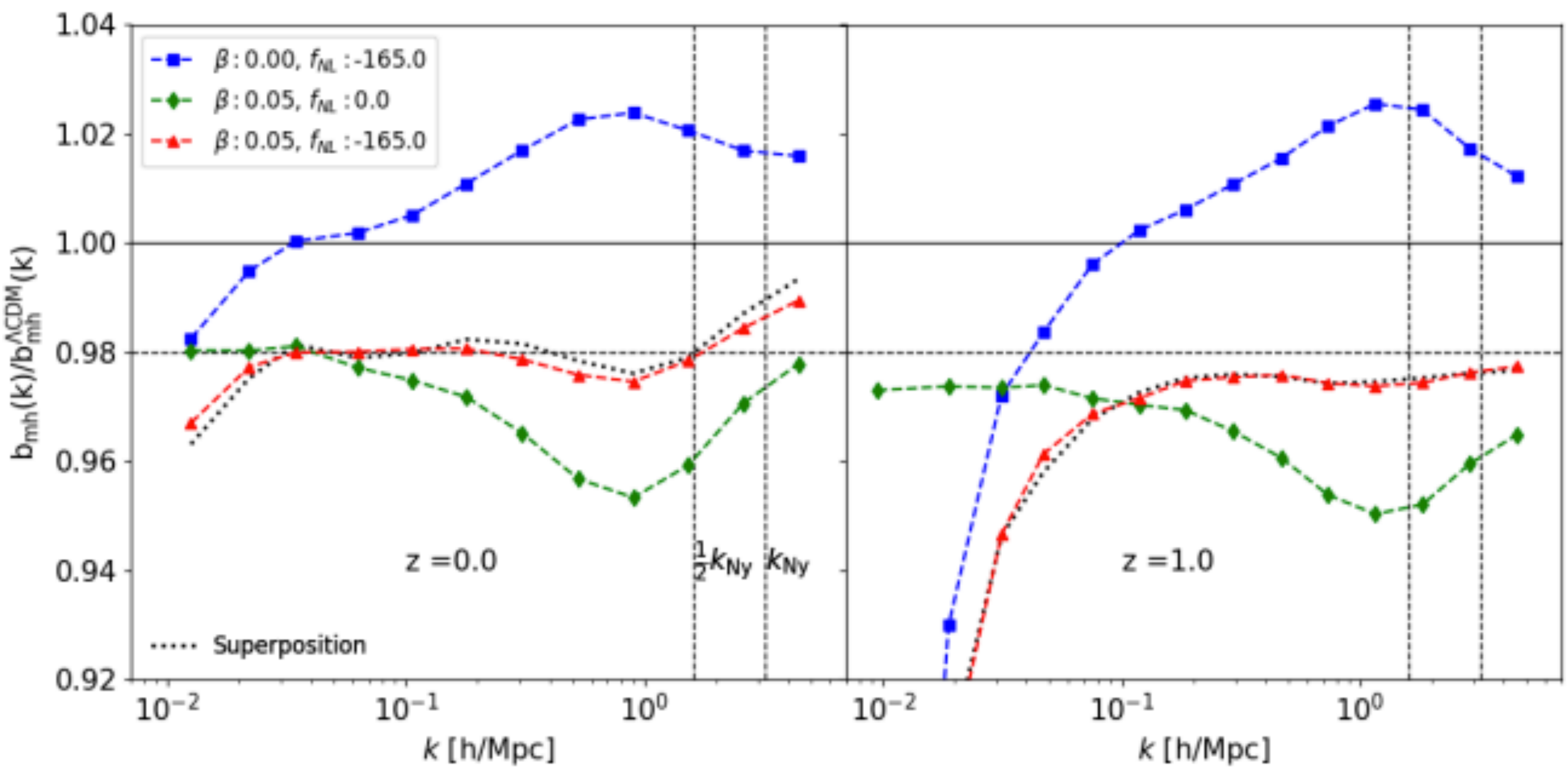

Figure 4. As in Fig. 3, for the halo-matter bias. Clearly, IDE shows no sign of scale-dependence on large scales.

$$b_{hm}(k) = \frac{P_{hm}(k)}{P_{mm}(k)}.$$

arXiv:1806.02356

Cairo, 2022

Halo Mass Function

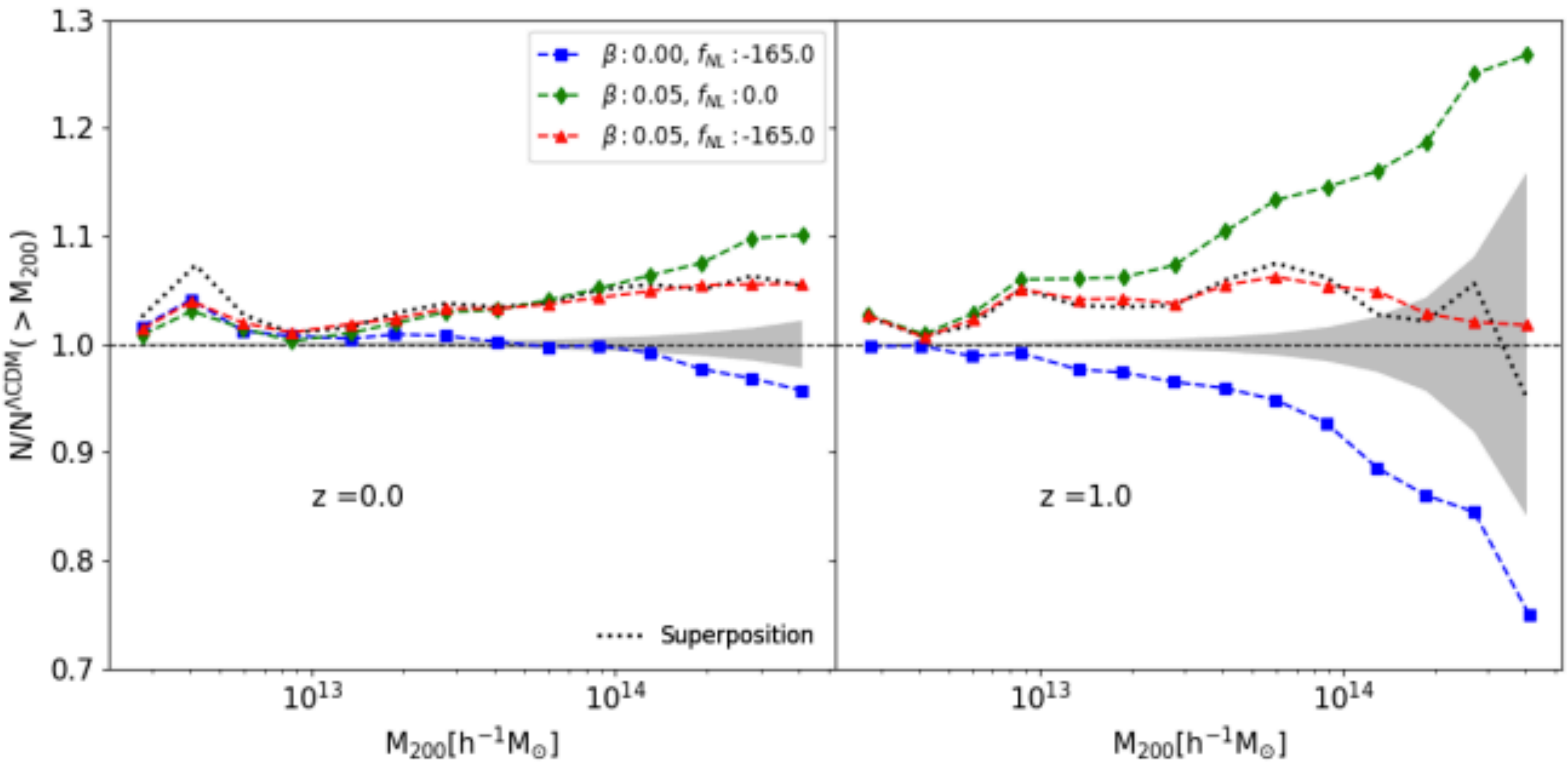

Figure 5. As in Fig. 3, for the halo mass function. The grey region represents the propagated Poissonian error of the number counts of halos in each bin.

arXiv:1806.02356

Cairo, 2022

Halo Concentration

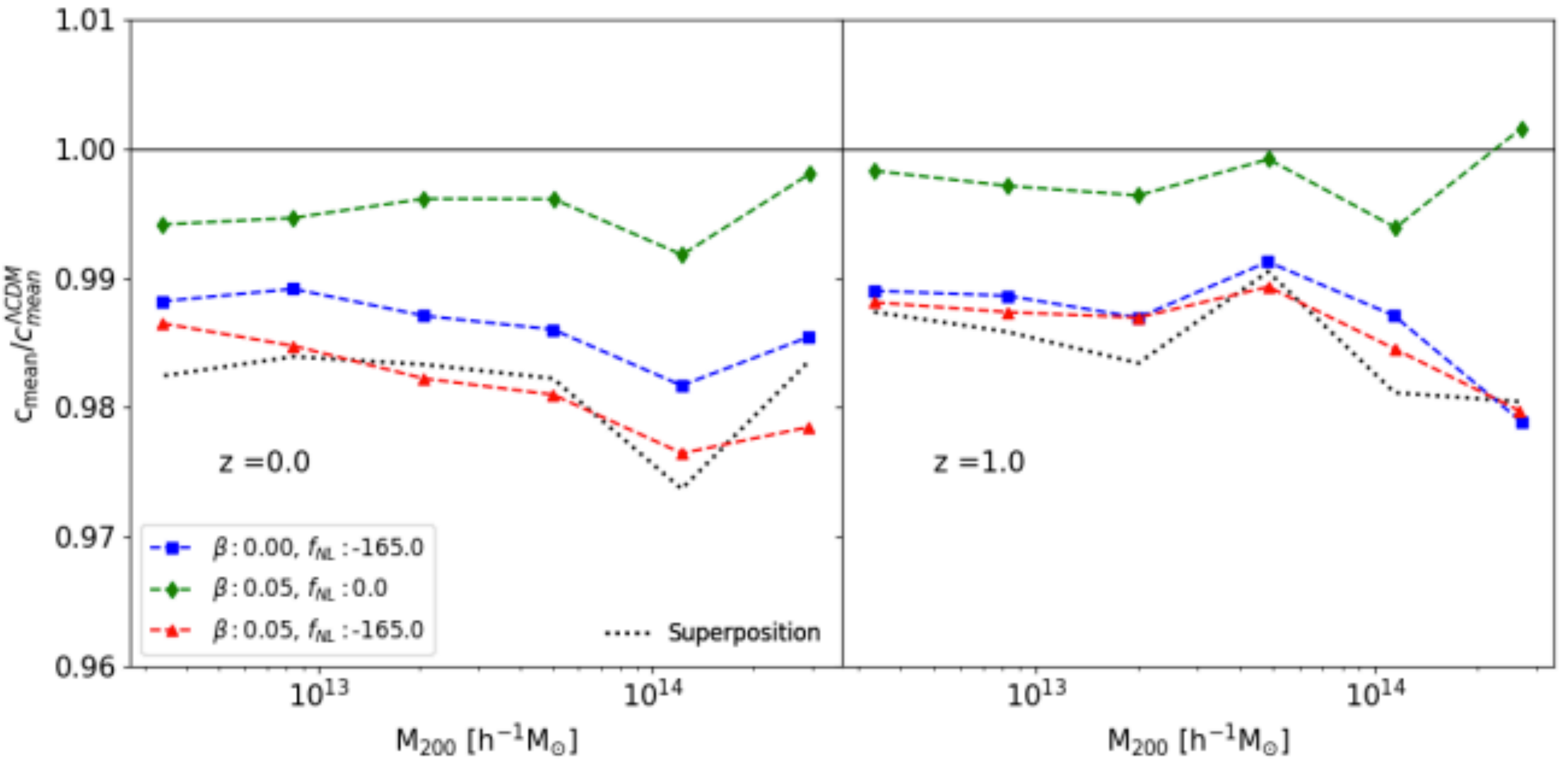

Figure 7. As in Fig. 3, for the concentration-mass relation.

$$\delta_c = \frac{200}{3}\frac{c^3}{\ln(1+c) - c/(1+c)} = 14.426\left(\frac{V_{max}}{H_0 r_{max}}\right)^2$$

arXiv:1806.02356

Cairo, 2022

sub-Halo mass function

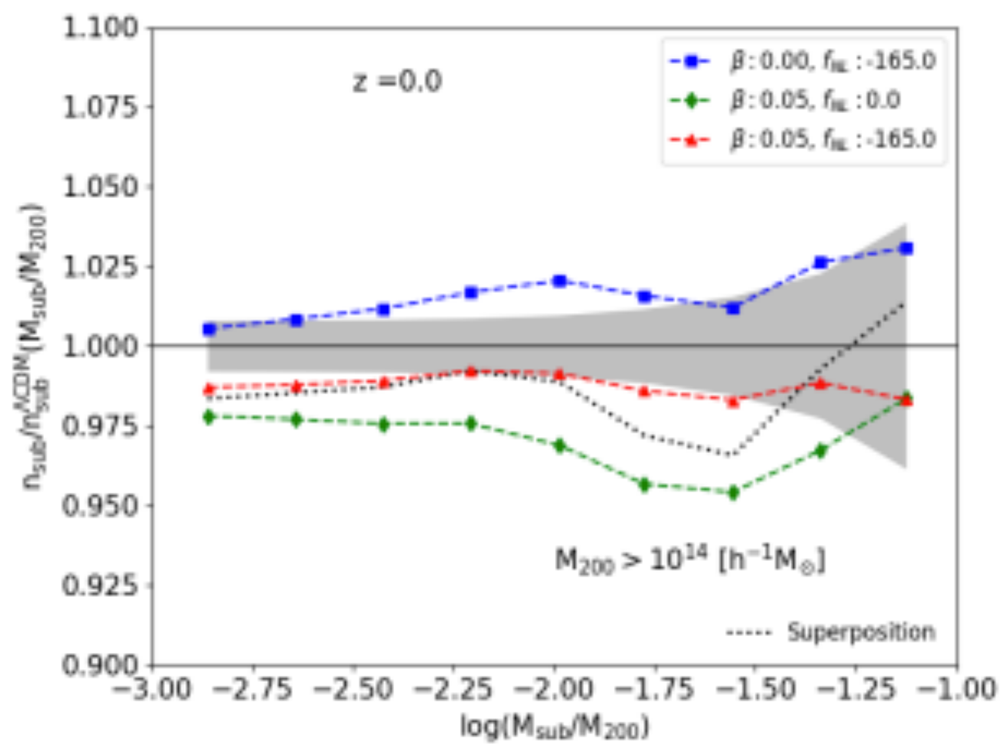

Figure 6. The subhalo mass function for the cosmologies under investigation at $z = 0$. The grey region represents the propagated Poissonian error of the number counts of subhalos in each bin and the dotted black line represents the superposition of IDE and PNG models.

arXiv:1806.02356

Cairo, 2022

void number function

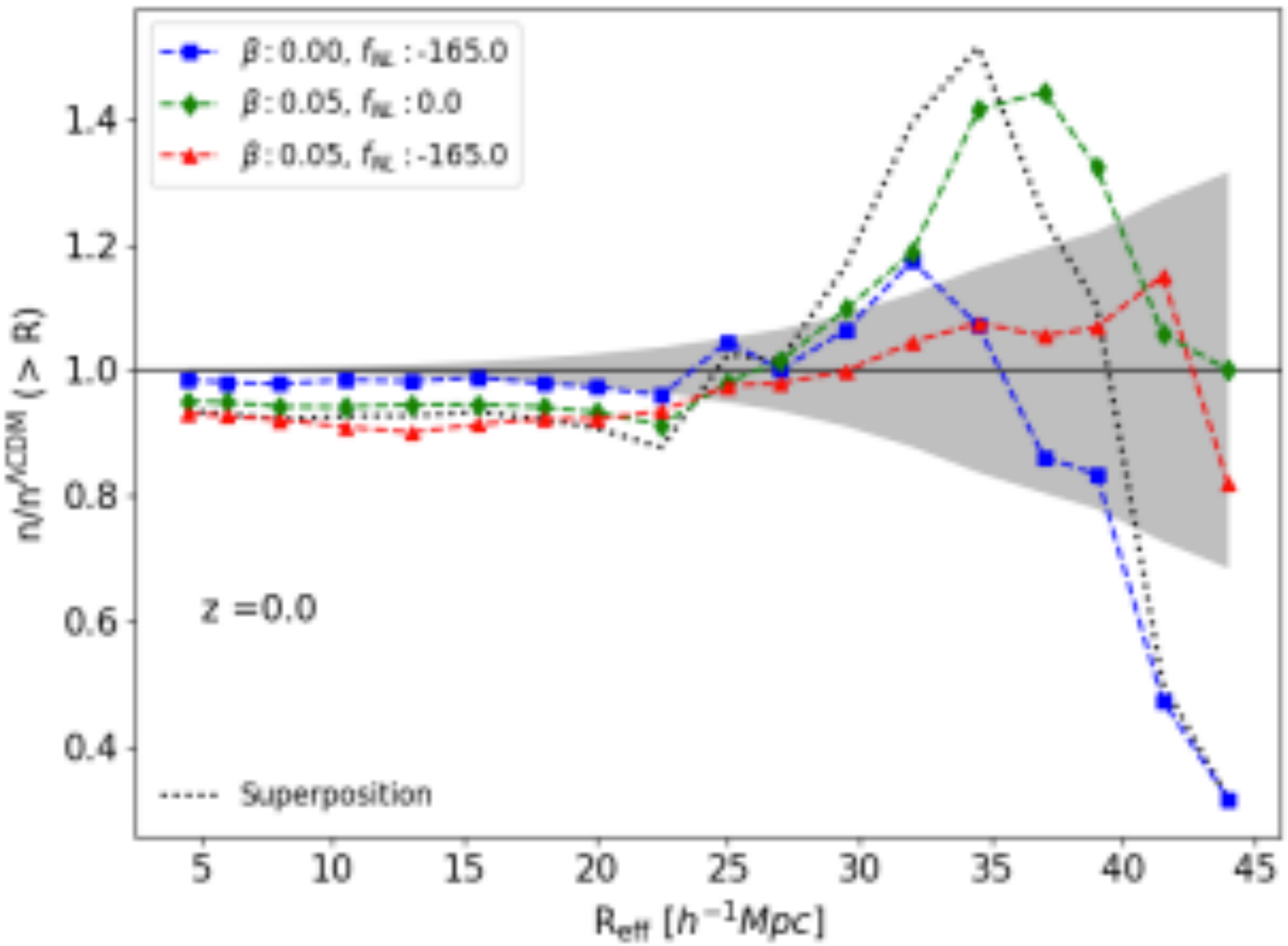

Figure 8. As in Fig. 6, for the void number function.

arXiv:1806.02356

Cairo, 2022

Conclusions

- IDE is not ruled out by current observations.

- LPT shows degeneracy on very large scales of the power spectrum between PNG and IDE.

- According to N-Body simulations, PNG and IDE also show some degeneracy on nonlinear power spectrum, halo mass function and nonlinear halo bias however it defies on halos structure properties such as Concentration.

- Disentangling PNG-IDE degeneracy could be done either by measuring degenerate observables at higher redshifts or by considering non-degenerate observables such as halo Concentration.